Gas Flow Dependence for Plasma-Needle Disinfection of *S. mutans* Bacteria

J Goree[1], Bin Liu[1], and David Drake[2]

[1] Department of Physics and Astronomy, The University of Iowa, Iowa City, IA 52242 USA
[2] Dows Institute for Dental Research, Dept. of Endodontics, College of Dentistry, The University of Iowa, Iowa City, IA 52242 USA

Abstract

The role of gas flow is studied and transport mechanisms are identified for the killing of bacteria by plasma needle treatment. The plasma needle is a small low-power impinging jet of weakly-ionized ionized helium at atmospheric pressure. This non-thermal glow discharge plasma kills bacteria, which in this case was *Streptococcus mutans* (*S. mutans*). A culture of *S. mutans* was plated onto the surface of agar, and spots on this surface were then treated with plasma. Afterwards, the sample was incubated and then imaged. These images, which serve as a biological diagnostic for characterizing the plasma, show a distinctive spatial pattern for killing that depends on the gas flow rate. As the flow is increased, the killing pattern varies from a solid circle to a ring. Images of the glow reveal that the spatial distribution of energetic electrons corresponds to the observed killing pattern. This suggests that a bactericidal species is generated in the gas phase by energetic electrons less than a millimeter from the sample surface. Mixing of air into the helium plasma is required to generate the observed O and OH radicals gases in the flowing plasma. Hydrodynamic processes involved in this mixing are buoyancy, diffusion and turbulence.

PACS: 52.80.-s 51.20.+d 47.54.Fj 47.27.wg 87.50.-a

1. Introduction

In a recently-reported experiment, a plasma-needle glow discharge was used to disinfect *Streptococcus mutans* (*S. mutans*) bacteria [1]. The "plasma needle" device that was used is intended for dental or medical applications [2-10]. It produces a small-diameter low-power non-thermal atmospheric-pressure glow discharge. A radio-frequency high voltage is applied to a needle-shaped electrode located inside a concentric gas-flow nozzle. The nozzle has a diameter of a few millimeters, and the plasma that flows out of the nozzle has a comparable diameter. Like other atmospheric glow discharges intended for sterilization of microorganisms [11-15], the plasma needle produces short-lived chemical species, which are propelled by the low-temperature gas toward a surface that is to be treated. The short lifetime of these species is an attractive feature of plasma treatment. For biomedical applications, the short lifetime assures that the active species do not remain after the treatment is completed.

The small size of the plasma needle device allows site-specific disinfection of spots with a diameter of a few millimeters without applying excessive heat to the biological sample. One proposed application for the plasma needle is the treatment of dental caries [5].

The most important bacterium for causing caries is *Streptococcus mutans*, or *S. mutans*. It colonizes smooth surfaces and fissures in teeth. Its temperature range for growth is 30° C to 47° C, with optimal growth at human body temperature, 37 ° C. Heat kills *S. mutans* at temperatures above 60 ˚C [16].

It has not yet been determined exactly which species produced by a plasma needle is most responsible for the bactericidal effect, or where it is formed [1]. As a step toward gaining such an understanding, we present here additional phenomenological results from the same experiment as in [1]. In that paper, the authors, working with Eva Stoffels, reported that the plasma needle is capable of killing *S. mutans* under conditions that are attractive to dentistry, with a treatment time of tens of seconds and with reproducible killing results. The method of sample preparation and analysis yielded images showing where the bacteria were killed on the treated surface. These images serve as a biological diagnostic of the plasma. Also reported were images of the glow above the sample. The significance of the glow is that it is produced by electron-impact excitation due to energetic electrons, and these same energetic electrons are capable of producing gas-phase species responsible for the observed bactericidal effect. These agents are O or OH formed in the gas phase, or metastable He.

The latter would be formed in the gas phase and subsequently enter the aqueous sample and dissociate H_2O to form OH *in situ*. Presently it is not determined yet which of these agents is responsible for the observed killing.

Three characteristic shapes for the killing spot were reported in [1]. These correspond to conditions termed cool, warm and hot. Cool conditions (which are typical for low voltages, short treatment times and large needle-to-sample separations) yield a killing pattern that is a uniform circle. This shape would be desirable for clinical applications. Hot conditions (which are typical for high voltages, long treatment times and small needle-to-sample separations) yield a killing pattern that is a concentric pattern: a circular spot where bacteria were killed, surrounded by a ring where there was little killing, surrounded by an outermost ring where the bacteria were killed. Warm conditions, which are intermediate to the cool and hot conditions, yield a ring-shaped killing pattern as for the hot conditions, but without the central spot.

In this paper, we report how the shape of the killing spot, and the shape of the plasma glow, depend on gas flow. These results are from the same experiment as in [1].

Features of plasma needle operation that make it attractive for possible dental applications include its ability to:

- perform site-specific disinfection, with small killing spots
- produce short-lived bactericidal species that would not remain in the mouth after treatment
- carry out this treatment in less than a minute with reproducible results
- treat without excessive heat.

For the latter requirement, tests have been reported that show that the plasma needle can be operated at a low enough power that sample temperatures do not rise to levels that would cause pulpal necrosis [5] or killing of bacteria by heat [1]. Here we report further tests as a step toward identifying the physical transport processes that are responsible for determining the killing spot size and shape.

2. Procedure

The experimental apparatus and procedure was previously described in [1], so that here we provide only a brief review.

Bacteria culture was plated on agar plates. The procedure for preparing these plates began with filling plastic Petri dishes to a depth of 4 mm with agar. This agar was then inoculated with *S. mutans* using a spiral-plating technique. The bacterial concentration was 10^6-10^7 colony-forming units per milliliter suspension. The resulting spiral-shaped line formed a bacterial lawn covering the surface of the agar.

The plasma needle device, which is similar to the design reported in [5], consists of a handpiece, a gas supply, and a high-frequency generator. The handpiece, figure 1(a), has three fittings: a gas inlet, an electrical feedthrough, and a nozzle. At the center of the nozzle is a tungsten neurology needle, with a diameter of 0.2 mm and a pencil-shaped taper of length 0.6 mm. The needle was concentric with a cylindrical glass tube nozzle, with an inside diameter D = 4 mm and an outside diameter of 6.35 mm. A glow formed at the tip of the tungsten needle, and at high powers it also formed along a portion of the needle's shaft, which was exposed for a length L = 5.7 mm. The nozzle was flush with the needle tip. The needle electrode was powered by 7.17 MHz radio-frequency high voltage. Our voltage was measured at the handpiece using a high-voltage probe and an oscilloscope. The gas used was pure helium.

Gas flow from the nozzle is important for several reasons. First, using gas flow is helpful in achieving breakdown, as compared to operating without any gas flow. Second, the flow mixes downstream from the nozzle with atmospheric gases including N_2, O_2 and H_2O, entraining these gases into the electron-rich flow so that radicals such as O and OH can be formed due to collisions with electrons. Third, the gas flow propels radicals and metastables toward the surface to be treated. Fourth, the diameter of the flow helps to define the diameter of the treated spot on the sample, which is an important parameter for biomedical applications.

We imaged the glow under the same operating conditions as for bactericidal treatment, but with the plasma impinging on a glass plate substituted for the agar. The brightness in the image reveals the presence of energetic electrons, which can also dissociate molecules to form radicals. To reveal the true profile of the intensity, we transformed the images using Abel inversion. To compute the emission function $I(r,z)$, we used the reverse Abel transform,

$$I(r,z) = -\frac{1}{\pi}\int_r^\infty \frac{di(x,z)}{dx}\frac{dx}{\sqrt{x^2-r^2}}\,, \qquad (1)$$

which assumes a circularly symmetric plasma. Here, $i(x,z)$ is the image as recorded by the camera, which had a linear response to intensity i. In practice the integral is performed not to an infinite distance but rather to the maximum distance x in the image. We averaged several consecutive video images to reduce the effect of noise when using equation (1).

After plasma treatment, samples were incubated so that visible colonies formed. The dishes were then illuminated with white light and imaged with a digital color camera. The lawn of bacterial colonies changed color and became visible to the naked eye after incubation. Light brown indicates living colonies, whereas dark brown indicates an absence of living colonies.

For the results presented here, the peak-to-peak voltage was 800 V, the separation between the needle and the sample was d = 3 mm, and the plasma was applied to the sample for an exposure time of 30 s. The primary parameter that was varied here was the flow rate. Results for varying the other parameters (voltage, separation and exposure time) were reported in [1].

3. Results

3.1. Microbiology

Images of the killing spots are shown in figure 2. These images show that the killing spot is 5 mm diameter, and it has a shape that depends strongly on the rate of gas flow. These images serve a dual role: they are a biological diagnostic of the plasma, and they indicate the efficacy of a treatment method.

The features seen in the images are explained here. The pattern of wavy lines of width 1 mm is due to the stylus that applied the bacterial suspension to the agar during the inoculation step. This pattern is not significant. What is significant is the round pattern of darkness centered in each image. A black color indicates an absence of living bacteria, whereas a light brown color indicates living bacteria. Color is the primary indicator for our bacteriology tests. We did not attempt to quantify the killing, for example by determining numbers of colony forming units. Instead, for our purposes here, we are interested in the shape of the killing spot.

Examining the sequence of images in figure 2, we can identify all three conditions: cool, warm and hot. These are described next.

At the lowest gas flow, 0.20 SLPM, the killing spot is a homogeneous circle. At 0.40 SLPM the killing pattern is nearly the same. A homogenous circle is the most desirable shape for clinical applications, where the practitioner would like to treat everything within a certain killing radius, and nothing outside it. In [1], the homogenous circular shape was described as the result of “cool” operating conditions. It was reported there that cool conditions are typical for low voltages, large needle-to-sample separations, and short treatment times. Here, we find that cool conditions are also typical for low gas flow rates.

Increasing the gas flow to 0.75 SLPM, the killing spot in figure 2 takes a new shape: a dark ring enclosing a dark spot. This shape was described in [1] as the result of “hot” operating conditions. Hot conditions were reported as being typical for high voltages, large needle-to-sample separations (which are conditions that bring the discharge near the glow-to-arc transition) and long treatment times. In [1] it was speculated that the central spot in the killing pattern might possibly be the result of a filament inside the glow, although no direct evidence of this was reported. We find that increasing the gas flow further to 1.25 and 1.50 SLPM, results in a similar “hot” pattern.

At the highest gas flow rates we tested, 3.0 and 4.0 SLPM, the killing pattern takes the third shape reported in [1]. This is the shape described as resulting from “warm” conditions. The killing occurs mainly in a ring, while bacteria in the center of the ring are mostly not affected by the treatment. A difference worth noting is that as one of the parameters was varied in [1], warm conditions were always found between the cool and hot conditions. Here, however, the “warm” shape arose at an extreme value of the gas flow. The killing spot made a transition from cool to hot to warm, rather than from cool to warm to hot. We also note that the tear-drop shape of the killing pattern at these high gas flow rates suggests that our impinging jet was not exactly circularly symmetric. Further experiments are needed to characterize the gas flow pattern, and to determine how stable it is.

3.2. Glow

Recall that the glow is produced by electron-impact excitation of gas atoms, so that it serves as a visual indicator of the presence of energetic electrons. These energetic electrons are also capable of generating radicals, either directly by dissociating gas molecules such as H_2O and O_2, or indirectly by generating metastable He atoms that might possibly enter a liquid and dissociate H_2O molecules in the liquid phase in the sample.

Side-view images are shown in figure 3. The left column shows the image as recorded by the camera, while the right column shows the Abel-inverted images. The latter are more instructive. For the high flows 0.75 – 1.50 SLPM that yield hot conditions, the glow spreads out much more than it does at cool and warm conditions, which were found at flow rates of 0.20 - 0.40 SLPM and 3.0 – 4.0 SLPM respectively. This result, that we observe more spread in the glow pattern for hot conditions, is consistent with the results reported in [1], suggesting that our identification of the cool, warm and hot regimes is appropriate for varying the gas flow as well as for the other parameters which were varied in [1].

The shape of the glow corresponds to the shape of the treatment spots. In figure 4, the Abel-inverted image of the glow is aligned with a corresponding image of the sample. For cool conditions in the left column, a glow shaped like a narrow column yields a treatment spot that is a homogeneous circle. For hot conditions in the right column, a glow that is ring-shaped near the sample yields a treatment spot that has a similar ring shape.

The spectrum of the glow emission is shown in figure 5. These spectra were recorded using an Ocean Optics HR2000 spectrometer with a 300 lines/mm grating. Because the spectrometer viewed the entire glow region downstream from the nozzle orifice, these spectra represent emission that is spatially averaged. The sensitivity of the spectrometer is peaked at about 400 nm and gradually diminishes by an order of magnitude for wavelengths between 400 and 900 nm. If we had corrected for this sensitivity, the oxygen lines in the infrared would appear much stronger than shown in figure 5.

Note that as the gas flow is increased, emission by the radicals O and OH is not greatly affected. The line emission intensity for nitrogen does diminish considerably at high flow rates, but not for the bactericidal radicals O and OH. The fact that the intensity of O and OH did not vary much suggests that the results for varying killing patterns we observed in figure 2 are not the result of an overall reduction in radical densities.

Table 1. Transit time *T* for the jet to flow a distance *d* = 3 mm, the Reynolds number *Re* computed using equation (2) assuming room temperature, and the Richardson number *Ri* computed using equation (3).

Gas flow (SLPM)	Nozzle velocity *V* (m/s)	Transit time *T* (ms)	*Re*		*Ri*
			for ν_{He}	for ν_{AIR}	
0.2	0.26	11.5	9	73	3.6
0.4	0.52	5.8	19	147	0.91
0.75	0.98	3.1	35	276	0.26
1.25	1.63	1.8	58	459	0.09
1.5	1.95	1.5	70	550	0.06
3.0	3.90	0.8	140	1099	0.016
4.0	5.2	0.6	186	1465	0.009

4 Discussion of Transport Processes

Here we discuss transport mechanisms in the flowing plasma.

4.1. Energetic electrons

There are three candidates for the agent responsible for the observed bactericidal effect: O or OH generated in the gas phase, or OH generated in the liquid phase due to metastable helium He* absorbed into the liquid from the gas. All three of these candidates require energetic electron impact. Metastable helium is produced by electron-impact excitation collisions. The radicals O and OH are also produced in the gas phase due to electron impact. (This could take place in a single step of electron-impact dissociation, or in a two-step process such as electron-impact ionization of H_2O followed by dissociation of H_2O^+ to produce OH, but in either case the process must begin with an electron-impact collision.) Energetic electrons are also responsible for producing the glow that we imaged.

Comparing two images, the glow and killing spot as in figure 4, can help in identifying the locations where the most important energetic electrons are produced. There is a strong correspondence in the shape of the glow and the shape of the killing spot. More specifically, it is the shape of the glow within a millimeter of the sample surface that dominates the shape of the observed killing spot. The ring-shaped pattern appears in the glow within the last millimeter before the flow impinges on the sample surface.

This result suggests that the agent responsible for the bactericidal is produced by electron impact within a millimeter of the sample surface.

We must next what transport mechanism is responsible for this length scale. One possibility is a finite lifetime of the species generated by electron impact. This species will be entrained in the gas flow, which is typically 1 m/s, or 1 mm/ms. Our observations of the ring in the glow and the killing pattern suggest that the last half millimeter of the flow is where the bactericidal agent is produced. This would, in turn, suggest that the agent has a lifetime of less than half a millisecond.

4.2. Decay of radicals

We have thus identified that a time scale of importance is the lifetime of the active agents produced by the plasma: OH, O and He^*. For OH, the lifetime in pure air at room temperature can be very short [17]. It is determined by the recombination reactions $OH + OH \rightarrow H_2O + O$ and $OH + OH + M \rightarrow H_2O + O + M$ where M is a collision partner such as N_2, O_2, or another gas molecule. The reaction rate will depend on the concentration of OH, and the reaction rate coefficient which has been reported [17] as $5 - 10 \times 10^{-12}$ cm^3 s^{-1} Depending on the OH concentration, recombination can happen as fast as 50 microseconds at room temperature [17]. An exact calculation of the radical lifetime would require a measurement of the OH concentration, which we have not made.

Comparing this time scale to the transit time *T* in Table 1 suggests that any OH radicals impinging on the sample must be produced less than a millimeter before the flow impinges on the surface. This is consistent with our result that the ring-shaped killing pattern indicates that the bactericidal agent is generated less than a millimeter before the gas impinges on the sample surface.

4.3. Hydrodynamic processes

4.3.1. Analogy to jet flames

The gas flow from the nozzle is, in the terminology of fluid mechanics, an “impinging jet”. The term “jet” describes the flow from a nozzle such as our cylindrical glass tube, and when it is directed toward a surface, it is said to be an “impinging jet.” The fluid mechanics literature for impinging jets includes, most abundantly, studies of combustion experiments with flames. In a jet flame, fuel from a nozzle mixes with ambient air. The plasma needle is analogous to a jet flame, with two notable differences. Firstly, instead of fuel we have energetic free electrons in the helium flow. Secondly, instead of a chemical reaction of fuel and air we have a physical reaction where the energetic electrons dissociate air molecules and excite He atoms to a metastable state.

This analogy suggests a need to identify the hydrodynamic transport processes that are responsible for mixing atmospheric gases including O_2 and H_2O into the flow and therefore into the glowing plasma. Once they are mixed into the glow, these gases are exposed to collisions with energetic electrons, which can then produce radicals such as O and OH.

Some of the key parameters in considering the transport problem are the flow’s velocity *V* and diameter *D* as well as the distance *d* between the nozzle and the sample. A significant time scale is the transit time for jet gas to flow to the sample, $T = d/V$. For transport to be effective, a molecule of ambient air must be transported radially a distance $D/2$ within a time *T*, as listed in Table 1.

4.3.2. Buoyancy

Buoyancy of helium can play a significant role in the transport, especially at low flow rates. The very low density of helium should cause it to rise, unless it is directed downward with a high momentum. A dimensionless parameter for comparing whether a flow is buoyancy-dominated or momentum-dominated is the Richardson number *Ri*

$$Ri = g D(\rho_\infty - \rho_{jet})/(\rho_{jet} V^2), \quad (3)$$

where g is the gravitation acceleration, D is the orifice diameter, and ρ is the mass density, specified separately for the jet fluid (helium) and the ambient gas at infinity (air) [18]. This is essentially a ratio of a potential energy due to gravity and a kinetic energy. The jet is classified as buoyancy-driven if $Ri > 1$, and as momentum-dominated if $Ri << 1$. We list values of *Ri* in Table 1.

Our lowest flow rates were characterized by $Ri > 1$. In this case, the downward flow has very little momentum, and buoyancy tends to cause helium to flow gently around the nozzle and then immediately upward. For the opposite case of $Ri << 1$, the helium streams vigorously toward the sample and impinges on the surface without any significant buoyancy effects. In our experiment, we varied the flow rate over a wide range, including both of these extremes. We can therefore conclude that future models of transport in this plasma must take buoyancy into account.

4.3.3. Turbulent mixing

Mixing is required, just as it is in the flame jet, and we must ask whether this mixing is dominated by diffusion or turbulence. If the flow is laminar, diffusion would be expected to play a dominant role in mixing H_2O and O_2 into the helium flow. Otherwise turbulent mixing would be expected to account for the mixing. This question is significant for the plasma needle because the formation of the radicals OH and O in the gas phase requires mixing air into the helium flow.

To estimate whether the flow was turbulent, we calculate the Reynolds number,

$$Re = DV/\nu, \quad (2)$$

where ν is the kinematic viscosity of the gas. For an impinging jet, it is common to choose values as follows: $D = 4$ mm is the inner diameter of the nozzle orifice, and V is the average velocity at the orifice. We report results computed two different ways: using the kinematic viscosity of He and air, which are respectively 1.04×10^{-4} m^2/s and 0.132×10^{-4} m^2/s. These values for viscosity, computed from standard values [18], are different by a large factor of 7.9, so that the reported value of the Reynolds number is very sensitive to this choice.

The computed values for *Re* are shown in Table 1. For example, we find $Re = 70$ for helium and $Re = 550$ for air, for a gas flow of 1.5 SLPM.

To determine whether these values are high enough to indicate turbulent flow, we must compare them to the critical value for the flow transition. This comparison is hindered, however, by a lack of data in the literature for the flow transition of an impinging jet of helium in air. The nearest two cases that we can find in the literature are an impinging jet with a single fluid, and a helium jet in open air. The transition occurs at markedly different values of *Re* for these two cases. For an impinging jet of a single fluid, the transition was reported at $Re = 50$ [19], while for an upward jet of helium into air it was $Re = 830$ [18]. For our flow, *Re* is generally between these two values, so that we are unable to conclude whether turbulent mixing occurred in our flow downstream of the nozzle orifice. Further experiments to detect fluctuations will be required to determine whether the flow is turbulent.

Regardless of whether the flow downstream of the nozzle orifice was turbulent, the flow inside the nozzle was probably stable. Flow inside a cylindrical pipe, i.e., Poiseuille flow, is known to be linearly stable to perturbations. Poiseuille flow exhibits a transition to turbulence only above a critical Reynolds number of at least 1760 [20].

4.3.4. Diffusive mixing

Diffusion will occur on a time scale r^2 / D_{diff} which depends on a characteristic distance r and a diffusion coefficient D_{diff}, but not on the flow rate. At sufficiently low flow rates one would expect there to be plenty of time for atmospheric gases to diffuse into the center of the helium flow. On the other hand, at high flow rates one would expect diffusive transport to be too slow, so that air would penetrate only to the edge of the flow by the time the flow impinges on the surface. This qualitative view seems to be consistent with the observations of the killing spot shape in figure 2: at the lowest flow rate the spot is uniform but at the highest flow rate it is a ring.

We can estimate the rate of diffusion. The diffusion coefficient for He in air at 293 K (i.e., slightly cooler than the room temperature in our experiment) is $D_{diff} = 0.58$ cm^2 s^{-1} [21]. For a laminar flow, the distance air must diffuse is the $r = 2$ mm radius of our helium flow. This would require a time scale $r^2 / D_{diff} = 69$ ms, which is at least an order of magnitude slower than the transit time T for the gas to flow from the nozzle to the sample. Therefore, only a very low concentration of air would mix all the way into the center of the helium flow, due to diffusion. This is not necessarily an indication that diffusion should be excluded, however, because Kieft *et al.* [9] reported that the concentration of air in the center of the flow from their plasma needle was indeed very low. It was too low to measure for their Raman scattering diagnostic, which had a detection limit of 0.5%. A more sensitive measurement of the concentration of air is required to determine whether diffusion alone can account for the transport.

5 Conclusions

We found that the plasma needle produces a killing pattern that varies strongly with the gas flow rate. The pattern is a desirable homogeneous circle at cool operating conditions achieved at low flow rates, but takes on a ring-shaped pattern at

higher flow rates. Images of the glow suggest that a ring-shaped killing pattern at a high flow rate corresponds to a ring-shaped spatial distribution of energetic electrons in the glow.

We discussed the transport mechanisms that could account for causing the observed killing pattern. Energetic electrons are required to generate bactericidal agents, and our results suggest that this generation occurs less than a millimeter from the sample surface. Finite lifetime of radicals together with the flow rate may determine the distance of the generation region from the sample. It is clear that buoyancy can be an important process at low flow rates. A mixing process introduces air into the electron-rich helium plasma. Identifying whether this mixing is dominated by diffusion or turbulence will require further investigations.

The transport processes we have discussed likely play a role not only in the plasma needle device that we used in our experiment, but also in other atmospheric-pressure plasmas. The “plasma pencil” device, for example, produces a similar low-power small-diameter plasma jet intended for biomedical applications [22].

Acknowledgments

We thank S. Clark, J. Marshall, V. Nosenko, F. Skiff, E. Stoffels, R. Vogel, and J. Wefel for useful discussions.

References

[1] Goree J Liu B Drake D and Stoffels E 2005 *IEEE Trans. Plasma Sci*. submitted
[2] Stoffels E, Flikweert A J, Stoffels W W and. Kroesen G M W 2002 *Plasma Sources Sci. Technol*. **11** 383
[3] Stoffels E Kieft I E and Sladek R E J 2003 *J. Phys. D* **36** 2908
[4] Sosnin E A Stoffels E Erofeev M V Kieft I E and Kunts S E 2004 *IEEE Trans. Plasma Sci*. **32** 1544
[5] Sladek R E J Stoffels E Walraven R Tielbeek P J A and Koolhoven R A 2004 *IEEE Trans. Plasma Sci*. **32** 1540
[6] Kieft I E, van der Laan E P and Stoffels E 2004 *New J. Phys.* **6** 149
[7] Kieft I E Darios D Roks A J M and Stoffels E 2005 *IEEE Trans. Plasma Sci.* **33** 771
[8] Sladek R E J and Stoffels E 2005 *J. Phys. D* **38** 1716
[9] Kieft I E, Van Berkel J J B N, Kieft E R and Stoffels E 2005 in *Plasma Processes & Polymers, Plasma Processes and Polymers* ed Riccardo d'Agostino, Pietro Favia, Christian Oehr and Michael R. Wertheimer (Weinheim Germany: Wiley VCH) 295
[10] Brok W J M, Bowden M D Van Dijk J, Van der Mullen J J A M and Kroesen G M W 2005 *J. Appl. Phys* **98** 013302
[11] Laroussi M 1996 *IEEE Trans. Plasma Sci.* **24** 1188
[12] Herrmann H W Henins I Park J and Selwyn G S 1999 *Phys. Plasmas* **6** 2284
[13] Montie T C Kelly-Wintenberg K and Roth J R 2000 *IEEE Trans. Plasma Sci*. **28** 41
[14] Laroussi M 2002 *IEEE Trans. Plasma Sci.* **30** 1409
[15] Vleugels M Shama G Deng X T Greenacre E Brocklehurst T and Kong M G 2005 *IEEE Trans. Plasma Sci.* **33** 824
[16] Ma Y and Marquis R E 1997 *Antonie Van Leeuwenhoek* **72** 91
[17] Ono R and Oda T 2003 *J. Appl. Phys*. **93** 5876
[18] Yildrim B S and Agrawal A K 2005 *Experiments in Fluids* **38** 161
[19] Unger D R and Muzzio F J 1999 *AIChE J*. **45** 2477
[20] Meseguer A 2003 *Phys. Fluids* **15** 1203
[21] Benenson W Harris J W Stocker H and Lutz H 2002 *Handbook of Physics* (New York: Springer-Verlag) p 249
[22] Laroussi M and Lu X 2005 *Appl. Phys. Lett*. **87** 113092

Figure 1.
Plasma needle setup. (a) The handpiece was a nylon Swagelok tee, with the nozzle pointed downward. (b) This drawing of the nozzle includes a sketch of the mixing region downstream from the nozzle orifice. The impinging jet was used to treat bacteria that were plated on the surface of the agar.

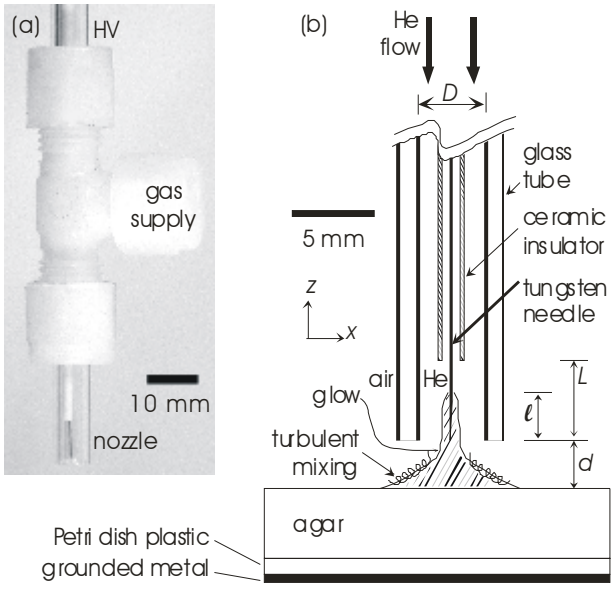

Figure 2.
Treatment spots on the Petri dish, imaged after incubation. A light color indicates living bacteria colonies. The wavy pattern is due to the inoculation method. A length scale is provided in the upper right. The killing pattern typically has a diameter of 5 mm. The shape of the pattern has a strong dependence on the gas flow rate.

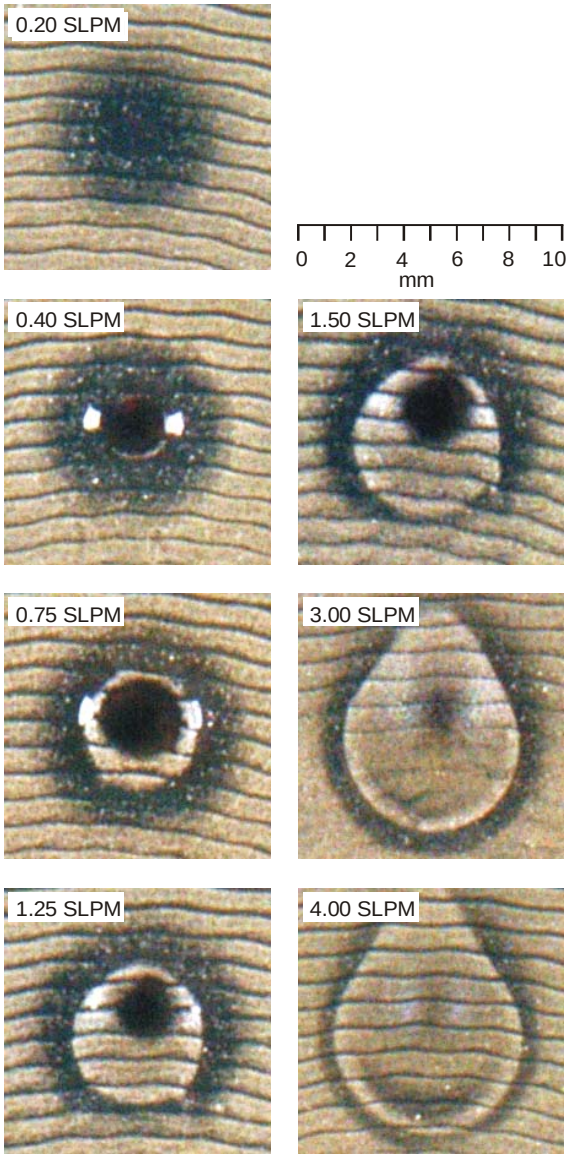

Figure 3.
Images of the glow as viewed from the side. The sample surface at the bottom, $z = 0$, was a glass plate substituted for the agar. The nozzle orifice at $z = 3$ mm is not visible in these images. The left column shows images as recorded by the camera, while the right column shows the corresponding images after Abel inversion, using equation (1), to reveal the radial distribution of the intensity.

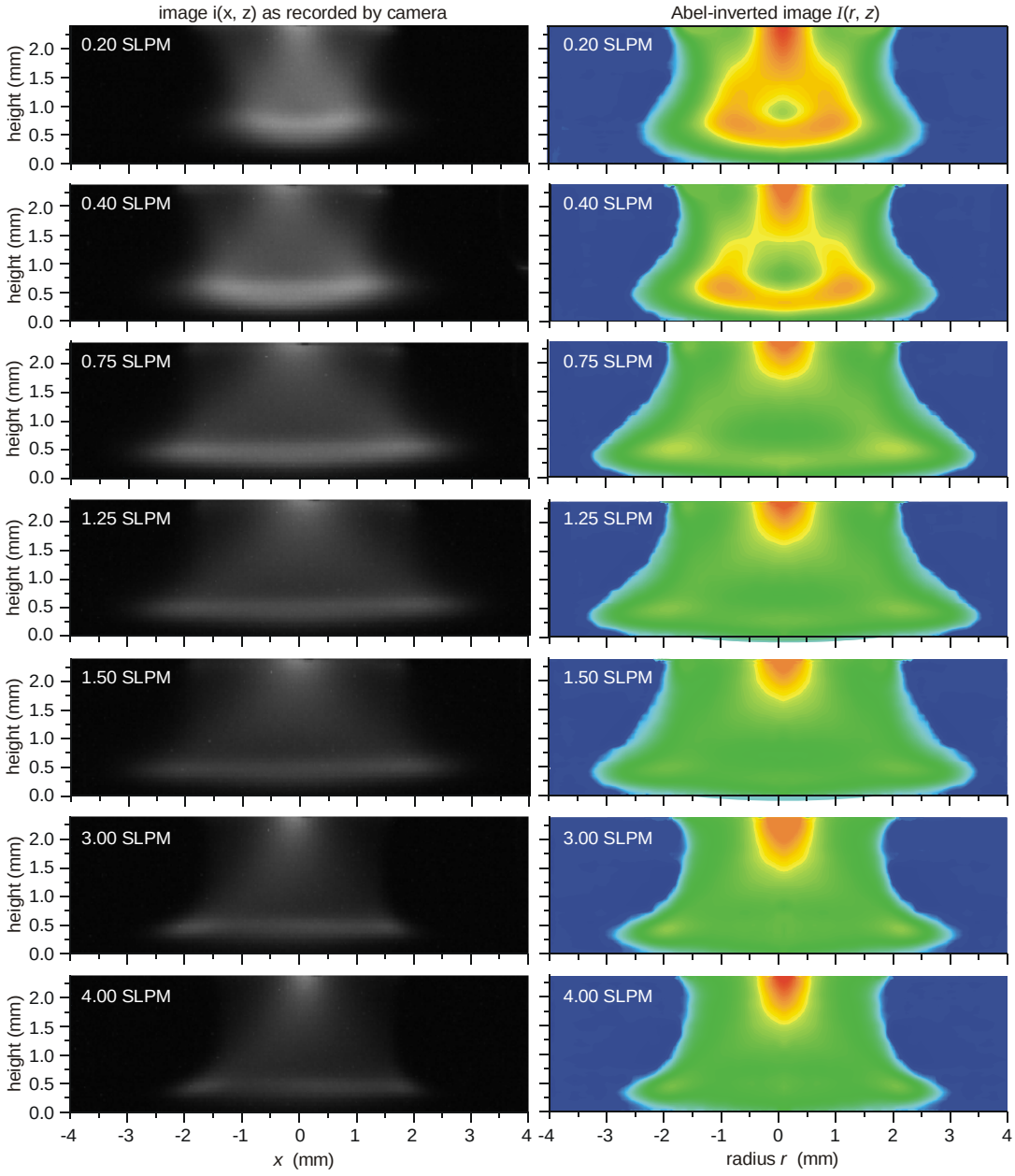

Figure 4.
Abel-inverted images (top) and images of spots on Petri dishes (bottom), at the same scale. For cool conditions (left column), the glow was a narrow column, yielding a killing pattern with a homogeneous circle of diameter 5 mm. For hot conditions (right column), the ring, with its 5-mm inside diameter, corresponds to a bright ring in the glow at r =2.5 mm and z = 0.5 mm. Comparing these images of the glow and the Petri dish helps explain the shape of the treatment spot.

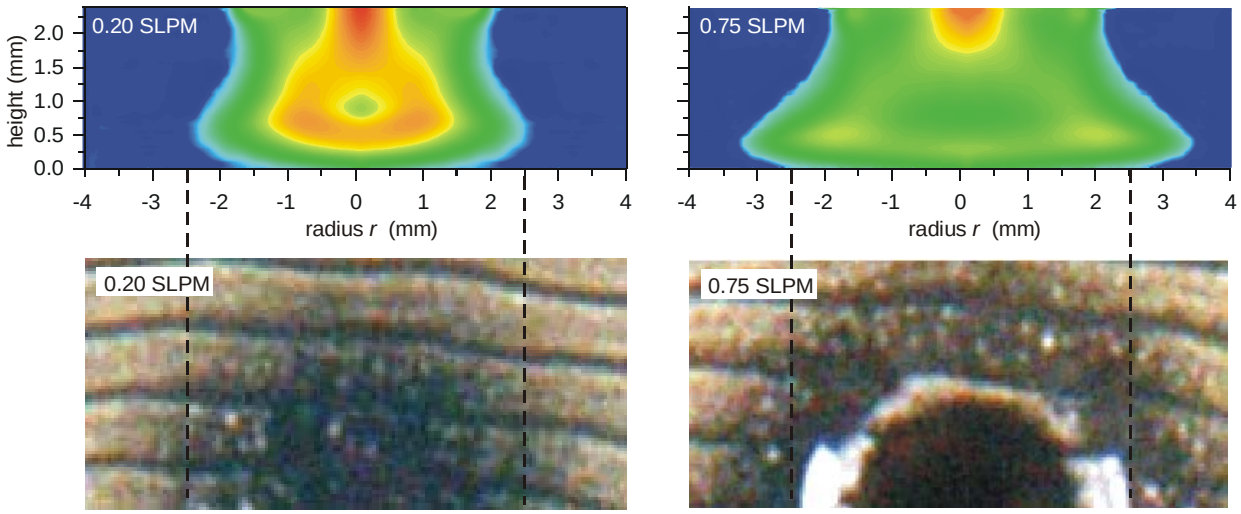

Figure 5.
Spectrum of the optical emission from the glow, downstream of the nozzle.